2018 European Control Conference (ECC)
June 12-15, 2018. Limassol, Cyprus

Robustification of the Synchronous Mode in a Hybrid Observer for a Continuous System under an Intrinsic Pulse-modulated Feedback

Diana Yamalova[1] and Alexander Medvedev[1]

Abstract— **The paper deals with a hybrid observer for an oscillating system composed of a linear continuous chain structure controlled by an intrinsic pulse-modulated feedback. The observed plant portrays a biochemical system under pulsatile regulation, e.g. an impulsive mathematical model of endocrine regulation. The observer reconstructs the continuous states of the model from only from the continuous system output and no measurements of the discrete part of the plant, i.e. the timing of the feedback firing events, are available. The problem of enlarging the basin of attraction of a synchronous observer mode that corresponds to a zero solution of the hybrid observer error is considered. It is demonstrated that the asymmetricity of the basin of attraction in the case of a static observer gain leads to a slow observer convergence and can be effectively alleviated through the introduction of a dynamical feedback.**

I. Introduction

Hybrid models, where continuous-time dynamics are admixed with discrete events, find a rapidly growing number of applications in life science and medicine [6],[1]. Complex nonlinear phenomena arising in such mathematical constructs are often too challenging to study in a general setting and finding subclasses of hybrid systems that lend themselves to analytical treatment is an important task.

In endocrine regulation, neural processes interact with the hormone kinetics thus giving rise to hybrid models with relatively slow continuous dynamics that are controlled through impulsive action of firing neurons [4], [5], [11]. An example of such a system is testosterone regulation in the male that has been intensively studied by means of a specialized version of Goodwin's oscillator called the Smith model [8], [9]. The mechanism of episodic secretion of the release hormones produced in the hypothalamus is typically described as pulse modulation, leading to a hybrid model called the impulsive Goodwin's oscillator [2].

The impulsive Goodwin's oscillator is characterized by two main features: a cascade structure of the continuous part of the model and a frequency and amplitude pulse-modulated feedback. While most of the continuous nonlinear oscillators produce self-sustained periodical solutions through Andronov-Hopf equilibrium-destabilizing bifurcations, the impulsive Goodwin's oscillator does not possess equilibria at all [2], [16]. Interestingly, the model has also been shown to describe actual endocrine data quite well, [7]. The pulse-modulated feedback of the impulsive Goodwin's oscillator is intrinsic, i.e. inaccessible for measurement, and poses a specific and seldom addressed in control theory problem of estimating discrete states of a hybrid system from only continuous measurements. This problem is more common in biomedical applications as measurements of discrete events are often not accessible in living organisms.

An observer making use of a single continuous output feedback for reconstructing the firing times and weights of the feedback pulses in the impulsive Goodwin's oscillator is proposed in [2]. For observer design, the hybrid state estimation problem is recast as a synchronization problem for the impulsive sequence of the plant and that of the observer. While being completely functional and able to handle both periodic and chaotic solutions in the plant, this observer structure suffers from slow convergence, especially in the case of periodic solutions of low multiplicity. To enhance observer convergence, an additional feedback of the (continuous) output estimation error is proposed in [13], [15], [14].

The present paper examines in detail a characteristic phenomenon arising in the latter observer, namely an asymmetric geometry of the basin of attraction of a synchronous mode, i.e. a zero solution to the hybrid estimation error dynamics. Even small overestimates of a plant feedback firing time lead to significantly prolonged observer transients while much larger underestimates can be promptly compensated for.

The main contribution of this work is thus the introduction of a dynamical feedback into the discrete part of the observer that alleviates the asymmetry and thus expedites the transient response to initial conditions mismatch.

The rest of the paper is composed as follows. First, the mathematical model of testosterone regulation given by the impulsive Goodwin's oscillator is briefly summarized. Then, the observer structure in hand is revisited. Further, local stability of the synchronous observer mode is analyzed and asymmetry of the basin of attraction is demonstrated. To alleviate this problem, a dynamical observer feedback is proposed and shown to improve observer convergence by extending the attraction of the synchronous mode to include overestimates of the firing time.

II. Impulsive model of testosterone regulation

Consider an impulsive mathematical model of testosterone (Te) regulation in the male with non-basal secretion. Besides Te, it involves two hormones: gonadotropin-releasing hormone (GnRH) and luteinizing hormone (LH). GnRH is released from the hypothalamus of the brain in pulsatile fashion with short latency. Reaching the pituitary gland,

* Supported by the Swedish Research Council, Grant 2015-05256
1 Information Technology, Uppsala University, SE-752 37 Uppsala, Sweden e-mail: diana.yamalova@it.uu.se, alexander.medvedev@it.uu.se

GnRH initiates the production of LH, which in turn stimulates production of Te in the testes. Finally, both the GnRH outflow and the LH secretion are subject to feedback inhibition by Te [10].

On the continuity intervals $t_n < t < t_{n+1}$, $n = 0, 1, 2, \ldots$, the model is given by the three ordinary differential equations

$$\begin{aligned} \dot{x}^{(1)}(t) &= -b_1 x^{(1)}(t), \\ \dot{x}^{(2)}(t) &= g_1 x^{(1)}(t) - b_2 x^{(2)}(t), \\ \dot{x}^{(3)}(t) &= g_2 x^{(2)}(t) - b_3 x^{(3)}(t). \end{aligned} \tag{1}$$

The continuous state variables correspond to the (bloodstream) concentrations of GnRH – $x^{(1)}$, LH – $x^{(2)}$, and Te – $x^{(3)}$. Here b_1, b_2, b_3, g_1, and g_2 are positive parameters, reflecting the kinetics of the involved hormones.

The action of the hypothalamic GnRH neurons can be described by a pulse modulator performing amplitude and frequency modulation, with the Te concentration as a modulation signal. Thus the discrete part of the model is

$$\begin{aligned} x^{(1)}(t_n^+) &= x^{(1)}(t_n^-) + \lambda_n, \quad x^{(2)}(t_n^+) = x^{(2)}(t_n^-), \\ x^{(3)}(t_n^+) &= x^{(3)}(t_n^-), \quad t_{n+1} = t_n + T_n, \\ T_n &= \Phi(x^{(3)}(t_n)), \quad \lambda_n = F(x^{(3)}(t_n)). \end{aligned} \tag{2}$$

The minus and plus in a superscript denote a left-sided and a right-sided limits, respectively, at the time instant t_n. Without loss of generality assume $t_0 = 0$. The functions $\Phi(\cdot)$ and $F(\cdot)$ stand for the frequency and amplitude characteristics, respectively, and parameterized by the Hill functions

$$\Phi(x^{(3)}) = \Phi_1 + \Phi_2 \frac{(x^{(3)}/h)^p}{1 + (x^{(3)}/h)^p}, F(x^{(3)}) = F_1 + \frac{F_2}{1 + (x^{(3)}/h)^p},$$

where the parameters $\Phi_1, \Phi_2, F_1, F_2, h$ are positive, and $p \geqslant 1$ is an integer. The choice of the modulation functions is in line with the physiological nature of the system, yielding smooth characteristics, bounded from above and below. It is straightforward to see that the following inequalities apply

$$0 < \Phi_1 \leqslant \Phi(\cdot) < \Phi_1 + \Phi_2, \quad 0 < F_1 < F(\cdot) \leqslant F_1 + F_2. \tag{3}$$

With the state vector $x(t) = [x^{(2)}(t) \quad x^{(2)}(t) \quad x^{(3)}(t)]^T$, model (1)-(2) can be rewritten as

$$\begin{aligned} \dot{x}(t) &= Ax(t), \quad y(t) = Lx(t), \\ z(t) &= Cx(t), \quad t_n < t < t_{n+1}, \end{aligned} \tag{4}$$

where

$$A = \begin{bmatrix} -b_1 & 0 & 0 \\ g_1 & -b_2 & 0 \\ 0 & g_2 & -b_3 \end{bmatrix}, \; L = \begin{bmatrix} 0 & 1 & 0 \\ 0 & 0 & 1 \end{bmatrix}, \; C = \begin{bmatrix} 0 & 0 & 1 \end{bmatrix},$$

$y(t)$ represents the measured hormone concentrations of LH and Te, and $z(t)$ is the hormone concentration that modulates the pulsatile feedback (Te). Obviously, A is Hurwitz, i.e. all its eigenvalues are negative real, which property simply corresponds to the fact that all organic molecules eventually decay. It is easy to check that (A, L) is observable.

The vector $x(t)$ experiences jumps at time instants t_n, when GnRH pulses are fired with the corresponding weights λ_n:

$$\begin{aligned} x(t_n^+) &= x(t_n^-) + \lambda_n B, \quad t_{n+1} = t_n + T_n, \\ T_n &= \Phi(z(t_n)), \quad \lambda_n = F(z(t_n)), \end{aligned} \tag{5}$$

where $B = \begin{bmatrix} 1 & 0 & 0 \end{bmatrix}^T$. Note that $CB = 0$, $LB = 0$, hence the outputs $y(t)$, $z(t)$ are continuous in t and have no jumps.

As shown in [2], the solutions to (4)–(5) are bounded and the system does not have equilibria. For biologically motivated parameter values, system (4)–(5) normally exhibits either a stable 1-cycle, or a stable 2-cycle (i.e. periodic solutions with either one or two GnRH impulses in the least period), but chaotic solutions are also possible.

The GnRH pulses are secreted at the time instants t_n with the weights λ_n and are immeasurable outside of the brain. Therefore, the state observation consists of producing estimates $(\hat{t}_n, \hat{\lambda}_n)$ of the impulse parameters (t_n, λ_n). Note that, with a completely known impulse sequence, estimates of the continuous state vector x can be obtained by conventional state estimation techniques.

III. Observer structure

In order to estimate the state vector of system (4),(5), a hybrid observer is introduced in [3] as:

$$\begin{aligned} \dot{\hat{x}}(t) &= A\hat{x}(t) + K(y(t) - \hat{y}(t)), \quad \hat{y}(t) = L\hat{x}(t), \\ \hat{z}(t) &= C\hat{x}(t), \quad \hat{t}_n < t < \hat{t}_{n+1}, \end{aligned} \tag{6}$$

$$\hat{x}(t_n^+) = \hat{x}(t_n^-) + \hat{\lambda}_n B, \quad \hat{t}_{n+1} = \hat{t}_n + \hat{T}_n, \quad \hat{\lambda}_n = F(\hat{z}(t_n)), \tag{7}$$

and

$$\hat{T}_n = \Phi\left(\hat{z}(\hat{t}_n) + k_f(z(\hat{t}_n) - \hat{z}(\hat{t}_n))\right). \tag{8}$$

The observer possesses two design degrees of freedom represented by the gains: The scalar gain k_f directly impacts the discrete dynamics of (6) while $K \in \mathbb{R}^{3\times 2}$ is responsible for continuous linear output error feedback to the estimates $\hat{x}(t)$. Notice that the observer is functional even with zero values of either gain. The case of $k_f = 0$ is considered in [3] and suffers from slow convergence. The continuous gain K is instrumental in assigning the convergence rate of the estimation error in the continuous states but not necessary as the matrix A is Hurwitz stable. In fact, even the gain matrices K that result in (slightly) non-Hurwitz matrices

$$D = A - KL$$

can still produce stable hybrid dynamics through the stabilizing action of k_f, as the separation principle does not apply.

The observer design described below is based on a local approach of assigning, through the output error feedback gains, a guaranteed convergence rate to the local dynamics of a zero solution of the hybrid state estimation error.

To completely characterize the hybrid system dynamics, not only the continuous state vector $x(t)$, but also the sequence of time instants t_n should be taken into account.

Let $(x(t), t_n)$ be a solution of plant equations (4), (5) with the parameters λ_k, T_k, and $x_k = x(t_k^-)$. Suppose that the

hybrid state $(x(t),t_n)$ is reconstructed by means of observer (6)–(8). Without loss of generality, assume that $t_0 \leqslant \hat{t}_0 < t_1$.

Obviously, the solution $(\hat{x}(t),\hat{t}_n)$ of observer equations (6)–(8) subject to the initial conditions $\hat{t}_0 = t_0$, $\hat{x}(\hat{t}_0^-) = x(t_0^-)$, yields $\hat{x}(t) = x(t)$ for all $t \geqslant t_0$. Such a solution $(\hat{x}(t),\hat{t}_n)$ is called *a synchronous mode* of observer (6)–(8) with respect to $(x(t),t_n)$, see [3]. Thus, a synchronous mode corresponds to zero dynamics of the hybrid observer.

A synchronous mode with respect to $(x(t),t_n)$ is called *locally asymptotically stable* (see [3]) if, for any solution $(\hat{x}(t),\hat{t}_n)$ of (6)–(8) such that the initial estimation errors $|\hat{t}_0 - t_0|$ and $\|\hat{x}(\hat{t}_0^-) - x(t_0^-)\|$ are sufficiently small, it follows that $\hat{t}_n - t_n \to 0$ and $\|\hat{x}(\hat{t}_n^-) - x(t_n^-)\| \to 0$ as $n \to \infty$. The latter implies $\hat{\lambda}_n - \lambda_n \to 0$ as $n \to \infty$.

Recall from [13] the Poincaré mapping capturing the propagation of the continuous plant and observer states through the discrete cumulative (plant and observer) sequence of the feedback firing instants

$$\begin{bmatrix}\hat{x}_{n+1}\\ \hat{t}_{n+1}\end{bmatrix} = Q(\hat{x}_n,\hat{t}_n) = \begin{bmatrix}P(\hat{x}_n,\hat{t}_n)\\ \hat{t}_n + \Phi(\alpha(\hat{x}_n,\hat{t}_n))\end{bmatrix}, \tag{9}$$

where $P(\hat{x}_n,\hat{t}_n) = P_{k,s}(\hat{x}_n,\hat{t}_n)$ with

$$\begin{aligned} P_{k,s}(\hat{x}_n,\hat{t}_n) &= \mathrm{e}^{A(\hat{t}_n+\Phi(\alpha(\hat{x}_n,\hat{t}_n))-t_s)}x(t_s^+)\\ &+ \mathrm{e}^{D\Phi(\alpha(\hat{x}_n,\hat{t}_n))}\left[\hat{x}_n + F(C\hat{x}_n)B - \mathrm{e}^{A(\hat{t}_n-t_k)}x(t_k^+)\right]\\ &- \sum_{j=k+1}^{s}\lambda_j \mathrm{e}^{D(\hat{t}_n+\Phi(\alpha(\hat{x}_n,\hat{t}_n))-t_j)}B, \end{aligned} \tag{10}$$

$R = (1-k_f)C$, $\alpha(\hat{x}_n,\hat{t}_n) = R\hat{x}_n + k_f z(\hat{t}_n)$ for any $n = 0,1,\ldots$, and indexes s, k ($k \leqslant s$) are such that $t_k \leqslant \hat{t}_n < t_{k+1}$, $t_s \leqslant \hat{t}_n + \Phi(\alpha(\hat{x}_n,\hat{t}_n)) < t_{s+1}$.

The synchronous mode with respect to the hybrid solution $(x(t),t_k)$ is completely characterized by the vector sequence (x_k,t_k). It is known from Theorem 2 in [12] that the mapping $Q(\hat{x}_n,\hat{t}_n)$ is smooth, which property allows for a linearization of the mapping Q in vicinity of (x_k,t_k). Denote the Jacobian of $Q(\cdot,\cdot)$ by $Q'(\zeta,\theta)$ at the point (ζ,θ), $\zeta \in \mathbb{R}^3$ $\theta \in \mathbb{R}$. If $\zeta = x_k$, $\theta = t_k$, then the Jacobian is calculated as

$$Q'(x_k,t_k) = J_k = \begin{bmatrix}(J_k)_{11} & (J_k)_{12}\\ (J_k)_{21} & (J_k)_{22}\end{bmatrix}, \tag{11}$$

where

$$\begin{aligned} (J_k)_{11} &= \Phi_k' A x_{k+1} R + e^{D\Phi(Cx_k)}\left(I + F_k' BC\right),\\ (J_k)_{12} &= Ax_{k+1}(1 + \Phi_k' k_f CAx_k) - e^{D\Phi(Cx_k)}\left(A(x_k + \lambda_k B)\right),\\ (J_k)_{21} &= \Phi_k' R, \quad (J_k)_{22} = 1 + \Phi_k' k_f CAx_k. \end{aligned}$$

Here Φ_k' and F_k' are shorthand notation for the derivatives $\Phi'(\alpha(x_k,t_k))$ and $F'(\alpha(x_k,t_k))$, respectively.

Consider a solution $(x(t),t_k)$ of system (4)–(5) satisfying $x_{k+1} \equiv x_k$, $\lambda_{k+1} \equiv \lambda_k$, $T_{k+1} \equiv T_k$ (1-cycle) and a synchronous mode of observer (6)–(8) with respect to $(x(t),t_k)$. Since $J_{i+1} \equiv J_i$, all the matrices in the sequence $\{J_i\}_{i=0}^{\infty}$ satisfy $J_i = J_0$. The following theorem provides a simple tool for checking local stability of the observer with respect to the solution in question.

Theorem 1 ([13]): Let the matrix J_0 be Schur stable, i.e. all the eigenvalues of this matrix lie strictly inside the unit circle. Then the synchronous mode with respect to $(x(t),t_k)$ is locally asymptotically stable.

Consider system (4), (5) with the following parameters:

$$b_1 = 0.012,\ b_2 = 0.15,\ b_3 = 0.1,\ g_1 = 2.8,\ g_2 = 1.5,$$

$$h = 2.7,\ p = 2,\ \Phi_1 = 40,\ \Phi_2 = 80,\ F_1 = 0.05,\ F_2 = 5.$$

Plant (4),(5) exhibits a stable 1-cycle (one firing of the pulse-modulated feedback in the least period of the solution) with

$$x_0^T = \begin{bmatrix}0.0516 & 1.0479 & 17.8606\end{bmatrix}^T.$$

Choose the observer feedback gain as

$$K = \begin{bmatrix}0 & 0.5 & 0\\ 0 & 0 & 0.5\end{bmatrix}^T.$$

A search for the value of k_f that minimizes the spectral radius of J_0 and, therefore, maximizes the convergence rate, results in $k_f = 59$. Fig. 1 illustrates the transients of the observer relative the transients of the plant, caused by a mismatch in the initial conditions of the plant and those of the observer, namely $\hat{t}_0 - t_0 = -40$, $\hat{x}_0 - x_0 = [-0.03, 0.5, 1.3]$.

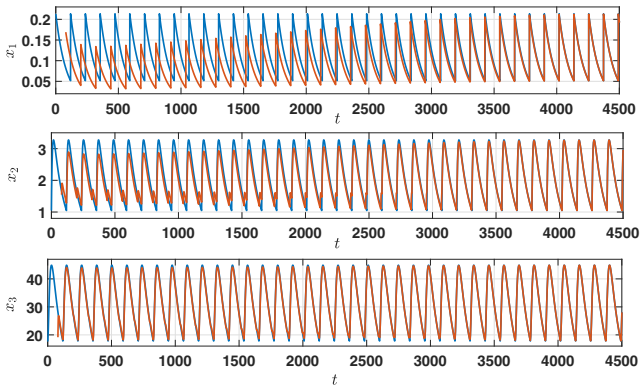

Fig. 1: Transients in the continuous states of the observer (in red) with respect to the corresponding plant states (in blue).

The considered observer design is clearly functional as the estimates of the continuous plant states converge to the actual values thus resulting in the output estimation error equal to zero. However, such an observer has the following drawback. Notice that the feedback in the discrete part of the observer is formed by output error: $k_f(z(\hat{t}_n) - \hat{z}(\hat{t}_n))$. The difference between the signals $z(t)$ and $\hat{z}(t)$ is depicted in Fig. 2. The vertical line corresponds to the plant firing time t_6. It can be seen that the rate of error change increases significantly immediately after the firing time. Hence, the convergence of the sequence $\{\hat{t}_k\}$ to the sequence $\{t_k\}$ from the right is much less robust than that from the left.

This can be confirmed in the following way. Consider the Jacobian $Q'(\zeta,\theta)$ in the vicinity of the point t_k with fixed $\zeta = x_k$. Denote $\varepsilon = \theta - t_k$. Note that Q' coincides with J_k for $\varepsilon = 0$. Consider the component $Q'^{(4,4)}$ of the Jacobian. This component corresponds to the dynamics of the discrete

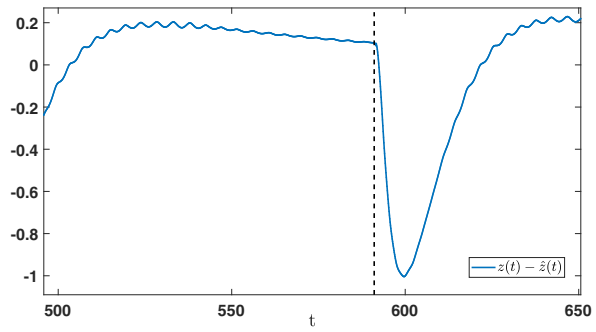

Fig. 2: The error $z(t)-\hat{z}(t)$

estimation error of the observer, i.e. the synchronization rate of the impulses. From Fig. 3, one can conclude that, for $\varepsilon > 0$, the change rate of $Q'^{(4,4)}(x_k,\theta)$ is much greater than for $\varepsilon < 0$.

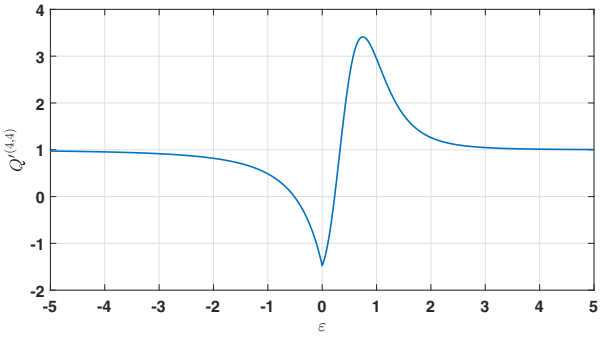

Fig. 3: The dependence of the component $Q'^{(4,4)}(x_k,\theta)$ on the time deviation $\varepsilon = \theta - t_k$

Since the element $Q'^{(4,4)}$ influences the spectral radius of Q' stronger than any other element, $\rho(Q')$ suitably increases for $\varepsilon > 0$ and almost instantly becomes greater than one (see Fig. 4) thus signaling loss of local stability.

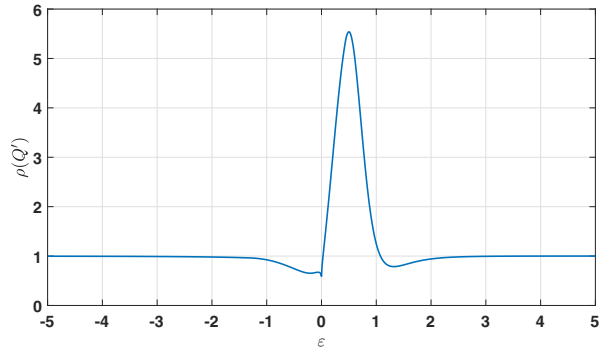

Fig. 4: The dependence of the spectral radius of the Jacobian $Q'(x_k,\theta)$ on the time deviation $\varepsilon = \theta - t_k$

Therefore, one can conclude that the basin of attraction of the synchronous mode in the vicinity of the point (x_k,t_k) is considerably asymmetrical. If, for some k, the point $\hat{t}_k$ is in a small right neighbourhood of t_k, i.e. $\hat{t}_k > t_k$, then the observer convergence is disrupted: The sequence will be shifted to the right by one feedback firing event, i.e. $(\hat{x}_k,\hat{t}_k) \to (x_{k+1},t_{k+1})$ that may increase the convergence time significantly, as illustrated by the following example.

Let $\hat{t}_0 - t_0 = 0.4$, i.e. the initial discrete error is 100 times closer to the synchronous mode than in the previous example. However, the initial point $\hat{t}_0$ is situated to the right of the point t_0. In Fig. 5, one can see that the points $(\hat{x}_k,\hat{t}_k)$ depart from (x_k,t_k) to (x_{k+1},t_{k+1}). As a result, the convergence of the observer to the synchronous mode becomes very slow (see Fig. 6).

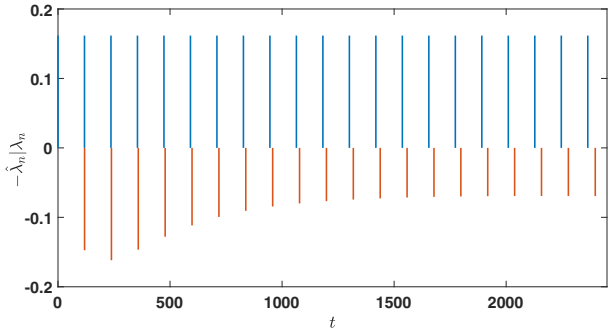

Fig. 5: Transients due to initial conditions mismatch in the firing times $\hat{t}_n$ and weights $\hat{\lambda}_n$ relative to t_n and λ_n: red lines (in the lower part of the figure) mark the firing times of the observer $\hat{t}_n$ with the height equal to $-\hat{\lambda}_n$. Blue lines (in the upper part of the figure) correspond to the pulse modulation of the plant in 1-cycle with the firing times t_n and the weights λ_n.

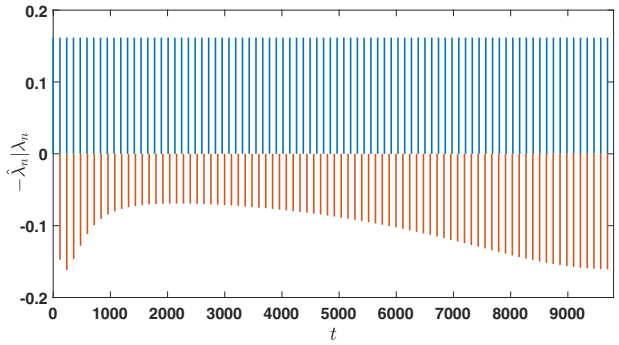

Fig. 6: Transients due to initial conditions mismatch in the firing times $\hat{t}_n$ and weights $\hat{\lambda}_n$ relative to t_n and λ_n. Blue lines - feedback firings in the plant (1-cycle), red lines - the estimates produced by the observer. The weights are depicted as amplitudes and taken with the opposite sign for the observer, to facilitate comparison.

IV. Dynamical observer feedback

In order to enlarge the basin of attraction of the synchronous mode in the vicinity of the point (x_k,t_k) for $\theta > t_k$

consider, instead of (8), a frequency modulation law in observer (6), (7) given by

$$\hat{T}_n = \Phi(\hat{z}(\hat{t}_n) + k_f r(\hat{t}_n)), \tag{12}$$

where $r(t)$ is a filtered version of the output estimation error $e(t) = z(t) - \hat{z}(t)$ governed by

$$\dot{r}(t) = -br(t) + ge(t), \quad r(t_0) = 0, \tag{13}$$

for some parameters $b, g > 0$.

Since (13) is linear, one has $r(t) = w(t) - \hat{w}(t)$, where

$$\dot{w}(t) = -bw(t) + gz(t), \tag{14}$$

$$\dot{\hat{w}}(t) = -b\hat{w}(t) + g\hat{z}(t), \tag{15}$$

and $\hat{w}(t_0) = w(t_0)$. Note that the discrete dynamics governing w can be obtained by sampling as

$$w_{k+1} = \mathrm{e}^{-b\Phi(z_k)} w_k + g \int_{t_k}^{t_{k+1}} \mathrm{e}^{-b(t_{k+1}-s)} z(s) ds.$$

Derive a discrete mapping describing the state evolution of the new observer. Denote $\xi(t) = \begin{bmatrix} x(t) \\ w(t) \end{bmatrix}$ and introduce the following matrices:

$$\bar{A} = \begin{bmatrix} A & \mathbf{0} \\ \bar{g} & -b \end{bmatrix}, \ \bar{g} = \begin{bmatrix} 0 & 0 & g \end{bmatrix}, \ \bar{B} = \begin{bmatrix} B \\ 0 \end{bmatrix}, \ \bar{C} = \begin{bmatrix} C & 0 \end{bmatrix},$$

$$\bar{L} = \begin{bmatrix} L & \mathbf{0} \end{bmatrix}, \ L_1 = \begin{bmatrix} 0 & 0 & 0 & 1 \end{bmatrix}, \ \bar{K} = \begin{bmatrix} K \\ \mathbf{0} \end{bmatrix}, \ \bar{D} = \bar{A} - \bar{K}\bar{L}.$$

For any $(\zeta, \theta) \in \mathbb{R}^4 \times \mathbb{R}$, introduce

$$\bar{\alpha}(\zeta, \theta) = \bar{R}\zeta + k_f L_1 \xi(\theta), \quad \bar{R} = \bar{C} - k_f L_1,$$

and select integers k and s, $k \leqslant s$, such that $t_k \leqslant \theta < t_{k+1}$, $t_s \leqslant \theta + \Phi(\bar{\alpha}(\zeta, \theta)) < t_{s+1}$. Define the function $\bar{P}(\zeta, \theta) = \bar{P}_{k,s}(\zeta, \theta)$ with

$$\begin{aligned} \bar{P}_{k,s}(\zeta, \theta) &= \mathrm{e}^{\bar{A}(\theta + \Phi(\bar{\alpha}(\zeta,\theta)) - t_s)} \xi(t_s^+) \\ &\quad + \mathrm{e}^{\bar{D}\Phi(\bar{\alpha}(\zeta,\theta))} \left[\zeta + F(\bar{C}\zeta)\bar{B} - \mathrm{e}^{\bar{A}(\theta - t_k)} \xi(t_k^+) \right] \\ &\quad - \sum_{j=k+1}^{s} \lambda_j \mathrm{e}^{\bar{D}(\theta + \Phi(\bar{\alpha}(\zeta,\theta)) - t_j)} \bar{B}. \end{aligned}$$

Theorem 2: A pointwise mapping for observer (6), (7), (12) is given by

$$\begin{bmatrix} \hat{x}_{n+1} \\ \hat{w}_{n+1} \\ \hat{t}_{n+1} \end{bmatrix} = \bar{Q}(\hat{x}_n, \hat{w}_n, \hat{t}_n) = \begin{bmatrix} \bar{P}(\hat{x}_n, \hat{w}_n, \hat{t}_n) \\ \hat{t}_n + \Phi(\alpha([\hat{x}_n; \hat{w}_n], \hat{t}_n)) \end{bmatrix}. \tag{16}$$

Proof: Denote $\hat{\xi}(t) = \begin{bmatrix} \hat{x}(t) \\ \hat{w}(t) \end{bmatrix}$. Then, it follows that

$$\dot{\xi}(t) = \bar{A}\xi(t), \quad \xi(t_n^+) = \xi(t_n^-) + \lambda_n \bar{B},$$

i.e. the continuous and discrete dynamics of the augmented system coincide with (4), (5) by replacing the vectors and matrices with the corresponding ones with ''bar''. The same applies to the observer.

Consider the difference $\Delta(t) = \xi(t) - \hat{\xi}(t)$ in the interval $(\hat{t}_n, \hat{t}_{n+1})$. Obviously, $\Delta(t)$ satisfies the linear differential equation $\dot{\Delta} = \bar{D}\Delta(t)$ at all the points t, where Δ has no jumps. Further, the function Δ undergoes jumps $\Delta(t^+) - \Delta(t^-) = \lambda_i \bar{B}$ at the points $t = t_i$, $k+1 \leqslant i \leqslant s$. Thus one concludes that

$$\Delta(\hat{t}_{n+1}^-) = \mathrm{e}^{\bar{D}\hat{T}_n} \Delta(\hat{t}_n^+) + \Delta_{k,s}, \tag{17}$$

where

$$\Delta_{k,s} = \sum_{i=k+1}^{s} \lambda_i \mathrm{e}^{\bar{D}(\hat{t}_{n+1} - t_i)} \bar{B}.$$

Now (17) can be rewritten as

$$\hat{\xi}_{n+1} = \xi(\hat{t}_{n+1}^-) + \mathrm{e}^{\bar{D}\hat{T}_n} (\hat{\xi}_n + \hat{\lambda}_n \bar{B} - \xi(\hat{t}_n^+)) - \Delta_{k,s}. \tag{18}$$

Since

$$\xi(\hat{t}_{n+1}^-) = \mathrm{e}^{\bar{A}(\hat{t}_{n+1} - t_s)} \xi(t_s^+), \quad \xi(\hat{t}_n^+) = \mathrm{e}^{\bar{A}(\hat{t}_n - t_k)} \xi(t_k^+),$$

equality (18) implies (16). ■

Theorem 3: The mapping $\bar{Q}(\zeta, \theta)$ is smooth.

Proof: Along the lines of Theorem 2 in [12]. ■

For an illustration of the observer performance, choose $b = 0.3$, $g = 0.2$, and $k_f = 85$. The value of the discrete observer feedback $k_f = 85$ is selected so that it minimizes the spectral radius of the Jacobian J_0.

As can be seen from Fig. 7, after a firing, the error $r(t)$ changes slower than the continuous output error $e(t)$, due to low-pass filtering. Hence, the proposed feedback structure with $k_f r(t)$ is expected to result in a more robust observer behavior. Naturally, a price to pay for it is a longer impulse response in the error signal. This would be a shortcoming in a purely continuous observer because of the slower convergence. In the case at hand, this actually brings about a convergence improvement as the discrete correction feedback has now access to a longer interval of non-zero values of the output error, i.e. $r(t)$ instead of $e(t)$, while the conditions of the synchronous mode are essentially the same.

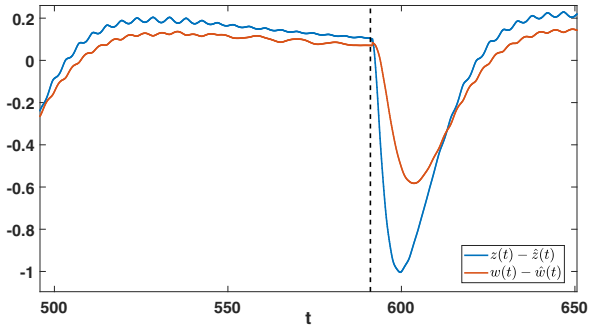

Fig. 7: The errors $z(t) - \hat{z}(t)$ and $w(t) - \hat{w}(t)$

Indeed, as seen in Fig. 8, the component $\bar{Q}'^{(4,4)}(x_k, w_k, \theta)$ changes more slowly in the vicinity of $\varepsilon = 0$ in comparison with $Q'^{(4,4)}(x_k, \theta)$.

As a result, the spectral radius of $\bar{Q}'(x_k, w_k, \theta)$ stays under one until $\varepsilon = 0.41$, see Fig. 9, thus implying stability of the synchronous mode for higher values of the estimation error. Therefore, one can conclude that the basin of attraction to the right of the point (x_k, t_k) for the proposed observer (6), (7), (12) is significantly larger than that for (6), (7), (8). This

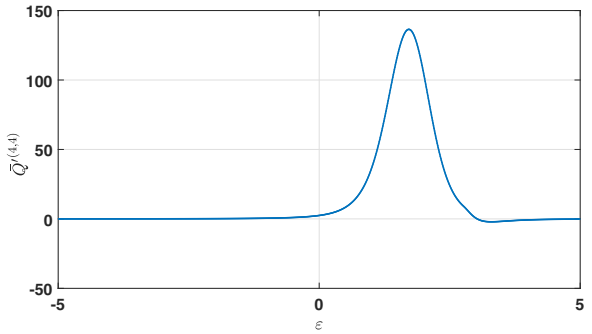

Fig. 8: The dependence of the component $\bar{Q}'^{(4,4)}(x_k, w_k, \theta)$ on the firing time estimation error $\varepsilon = \theta - t_k$.

means that, after the initial transient of the sequence $(\hat{x}_k, t_k)$ to (x_k, t_k), in the case of $\hat{t}_k$ "jumping" to the right of t_k, the discrete trajectory will not leave the neighbourhood where $\bar{Q}'(x_k, w_k, \theta) < 1$ and converge to the synchronous mode.

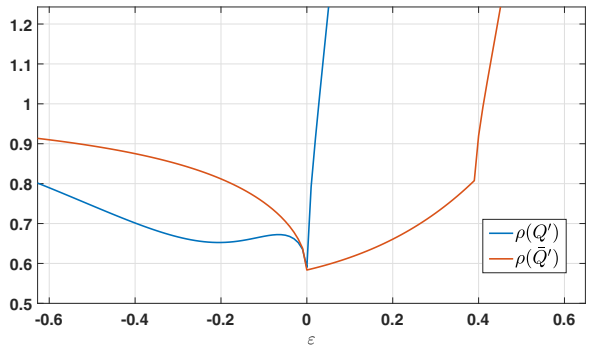

Fig. 9: The dependence of the spectral radii of the Jacobians $Q'(x_k, \theta)$ and $\bar{Q}'(x_k, w_k, \theta)$ on the time deviation $\varepsilon = \theta - t_k$

The desired behavior is confirmed in Fig. 10, where the considered above example is simulated with the initial error $\hat{t}_0 - t_0 = 0.4$. The trajectory does not leave the neighbourhood bounded by the initial error and the sequence $\{\hat{t}_k\}$ convergences to $\{t_k\}$ from the right.

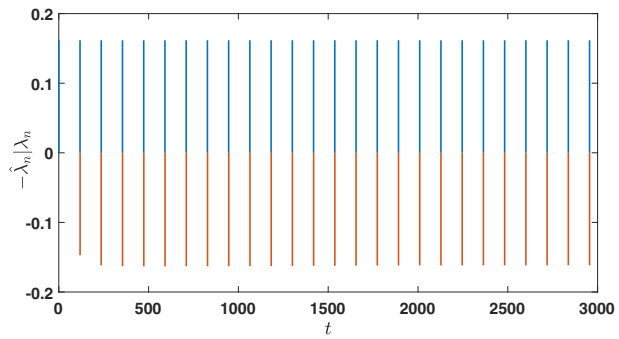

Fig. 10: Transients due to initial conditions mismatch in the firing times $\hat{t}_n$ and weights $\hat{\lambda}_n$ relative to t_n and λ_n

V. Conclusions

The basin of attraction of a synchronous mode of a hybrid observer for a continuous system under an intrinsic pulse-modulated feedback is investigated. Due to high nonlinearity of the observer error dynamics typical to impulsive systems, overestimation of firing events by the observer has more severe impact on the observer convergence than underestimation of those. The introduction of a dynamical feedback in the discrete part of the observer is proposed to alleviate the asymmetricity of the basin of attraction and shown to lead to improvement of the observer convergence time.

References

[1] K. Aihara and H. Suzuki. Theory of hybrid dynamical systems and its applications to biological and medical systems. *Philosophical Transactions of the Royal Society of London A: Mathematical, Physical and Engineering Sciences*, 368(1930):4893–4914, 2010.

[2] A. Churilov, A. Medvedev, and A. Shepeljavyi. Mathematical model of non-basal testosterone regulation in the male by pulse modulated feedback. *Automatica*, 45(1):78–85, 2009.

[3] A. Churilov, A. Medvedev, and A. Shepeljavyi. State observer for continuous oscillating systems under intrinsic pulse-modulated feedback. *Automatica*, 48(6):1005–1224, 2012.

[4] D. M. Keenan and J. D. Veldhuis. A biomathematical model of time-delayed feedback in the human male hypothalamic-pituitary-Leydig cell axis. *Amer. J. Physiology. Endocrinology and Metabolism*, 275(1):E157–E176, 1998.

[5] D.M. Keenan, I.J. Clarke, and J.D. Veldhuis. Noninvasive analytical estimation of endogenous GnRH drive: analysis using graded competitive GnRH-receptor antagonism and a calibrating pulse of exogenous GnRH. *Endocrinology*, 152(12):4882–4893, 2011.

[6] L. Mailleret and V. Lemesle. A note on semi-discrete modeling in the life sciences. *Phil. Trans. R. Soc. A*, 367(1908):4779–4799, 2009.

[7] P. Mattsson and A. Medvedev. Modeling of testosterone regulation by pulse-modulated feedback. In *Advances in Experimental Medicine and Biology: Signal and Image Analysis for Biomedical and Life Sciences*, volume 823, pages 23–40. Springer, 2015.

[8] W. R. Smith. Hypothalamic regulation of pituitary secretion of lutheinizing hormone—II Feedback control of gonadotropin secretion. *Bulletin of Mathematical Biology*, 42:57–78, 1980.

[9] W. R. Smith. Qualitative mathematical models of endocrine systems. *American Journal of Physiology*, 245(4):R473–R477, 1983.

[10] J. D. Veldhuis. Recent insights into neuroendocrine mechanisms of aging of the human male hypotalamic-pituitary-gonadal axis. *Journal of Andrology*, 20(1):1–18, 1999.

[11] J.D. Veldhuis, D.M. Keenan, and S.M. Pincus. Motivations and methods for analyzing pulsatile hormone secretion. *Endocrine Reviews*, 29(7):823–864, 2008.

[12] D. Yamalova, A. Churilov, and A. Medvedev. Hybrid state observer with modulated correction for periodic systems under intrinsic impulsive feedback. In *Proc. 5th IFAC International Workshop on Periodic Control Systems. IFAC Proceedings Volumes (IFAC-PapersOnline)*, volume 5, pages 119–124, 2013.

[13] D. Yamalova, A. Churilov, and A. Medvedev. Design degrees of freedom in a hybrid observer for a continuous plant under an intrinsic pulse-modulated feedback. In *Proc. 1st IFAC Conference on Modelling, Identification and Control of Nonlinear Systems. IFAC Proceedings Volumes (IFAC-PapersOnline)*, volume 48, pages 1080–1085, 2015.

[14] D. Yamalova, A. Churilov, and A. Medvedev. Hybrid observer for an intrinsic impulsive feedback system. *IFAC-PapersOnLine*, 50(1):4570 – 4575, 2017. 20th IFAC World Congress.

[15] D. Yamalova and A. Medvedev. Design of a hybrid observer for an oscillator with an intrinsic pulse-modulated feedback. In *2017 American Control Conference (ACC)*, pages 1175–1180, 2017.

[16] Zh.T. Zhusubaliyev, A. Churilov, and A. Medvedev. Bifurcation phenomena in an impulsive model of non-basal testosterone regulation. *Chaos*, 22(1):013121–1—013121–11, 2012.